Experimental Study of the Kinetics of the Reaction of Acetic Acid with Hydroxyl Radicals from 255 to 355 K

Yi-wen Huang,*,† Timothy J. Dransfield,*,‡ Jeremy D. Miller,‡ Ronny D. Rojas,‡ Xavier G. Castillo,‡ and James G. Anderson†

Department of Chemistry and Chemical Biology, Harvard University, 12 Oxford Street, Cambridge Massachusetts 02139, and Department of Chemistry, University of Massachusetts Boston, 100 Morrissey Boulevard, Boston Massachusetts 02125

Received: September 29, 2008; Revised Manuscript Received: November 17, 2008

The rate constant of the reaction of OH with acetic acid over the temperature range of 255−355 K was determined using our High-Pressure Flow System with laser-induced fluorescence detection of the OH radicals and FTIR spectrometry for acetic acid quantification. The rate constant displays a negative temperature dependence and can be described by the Arrhenius expression: $k_1(T) = (5.38 \pm 0.28) \times 10^{-14} \exp(740 \pm 51/T)$ cm^3 molecule^{-1} s^{-1}, with $k_1 = (6.77 \pm 0.14) \times 10^{-13}$ cm^3 molecule^{-1} s^{-1} at 295 K. The negative temperature dependence suggests a pre-reactive complex formation between the OH radicals and the acetic acid monomer, and this result is consistent with previous reports. The use of FTIR spectrometry allows for separation of the acetic acid monomer and dimer in the spectrum and gives a measurement of the acetic acid monomer that is independent of the temperature measurement and free of reliance on an equilibrium constant expression that can introduce high uncertainty. The highly sensitive laser-induced fluorescence for OH detection coupled with the FTIR spectrometry result in a rate constant measurement with low uncertainty, and the data set presented here in the temperature range of 255−355K serves to bridge existing data sets that are obtained either above or below room temperature.

Introduction

Oxygenated volatile organic compounds (OVOCs) are key trace species for the HO_x budget in the atmosphere, which controls the oxidative capacity of the troposphere and stratosphere. Among these compounds, acetic acid (CH_3COOH) has recently been identified as an important species in the troposphere. It is one of the most abundant carboxylic acids in the atmosphere, and it contributes significantly to the acidity of precipitation, especially in remote regions.[1] In the troposphere, acetic acid is mainly photochemically produced via reactions of peroxy acetyl radicals ($CH_3C(O)OO$) with peroxy radicals, HO_2 and CH_3O_2, which account for 60−70% of the global production of acetic acid.[2,3] There is a discrepancy in the estimated global photochemical source for acetic acid, ranging from 42 to 120 Tg yr^{-1}.[2,4,5] Direct biogenic emission from biomass burning contributes around 30% of the acetic acid production[3] and is estimated to be between 22 and 48 Tg yr^{-1}.[3,6] Other sources include soil and vegetation emissions,[7,8] vehicle exhausts,[9] and snow packs.[10] Because of its high solubility in water, a large portion of the emitted acetic acid is washed out from the lower troposphere. However, acetic acid can be directly transported to high altitudes by continental outflows and by vertical convection that couples the lower and upper troposphere. The mixing ratio in the tropical upper troposphere is measured to be as high as 2 ppbv.[11] This finding suggests that acetic acid could be a source as important as methane for methyl peroxy radicals in the upper troposphere.[11,12]

The predominant removal pathways of acetic acid are via dry and wet deposition. However, in the upper troposphere and lower stratosphere, the reaction with hydroxyl radicals (OH) is believed to be the major loss process for acetic acid. There are two possible hydrogen abstraction channels through which the reaction between CH_3COOH and OH could proceed.

$$CH_3COOH + OH \rightarrow CH_3 + CO_2 + H_2O \quad (1a)$$

$$\rightarrow CH_2COOH + H_2O \quad (1b)$$

These reaction rates have been studied under different experimental conditions. Zetzsch and Stuhl reported a rate constant $k_1 = (5.99 \pm 0.78) \times 10^{-13}$ cm^3 molecule^{-1} s^{-1} at 298 K between 20 and 500 Torr using flash photolysis coupled with resonance fluorescence to detect OH.[13] Dagaut et al. used flash photolysis with OH resonance fluorescence detection to measure the rate constants of OH radicals reacting with a series of carboxylic acids over a temperature range of 240−400 K and a pressure range of 25−50 Torr.[14] They found a positive temperature-dependent rate of $k_1(T) = (1.3 \pm 0.1) \times 10^{-12} \exp(-(170 \pm 20)/T)$ cm^3 molecule^{-1} s^{-1}. On the other hand, Singleton et al. investigated the temperature dependence of OH + CH_3COOH, using laser flash photolysis coupled with resonance absorption detection of OH and found a negative temperature dependence over a temperature range of 297−445 K at 500 Torr.[15] More recently, Butkovskaya et al. measured the rate in a high-pressure turbulent flow system using chemical ionization mass spectrometry for OH detection at 200 Torr over the temperature range of 229−300 K.[12] They observed a strong negative temperature dependence for this reaction and reported the Arrhenius expression: $k_1(T) = (2.2 \pm 0.2) \times 10^{-14} \exp((1012 \pm 80)/T)$ cm^3 molecule^{-1} s^{-1}, and the rate at 298 K is $(6.6 \pm 0.8) \times 10^{-13}$ cm^3 molecule^{-1} s^{-1}. In combination with the results

* To whom correspondence should be addressed. E-mail: ywhuang@huarp.harvard.edu (Y.-w.H.); timothy.dransfield@umb.edu (T.D.).
† Harvard University.
‡ University of Massachusetts Boston.

10.1021/jp808627w CCC: $40.75
Published on Web 12/19/2008

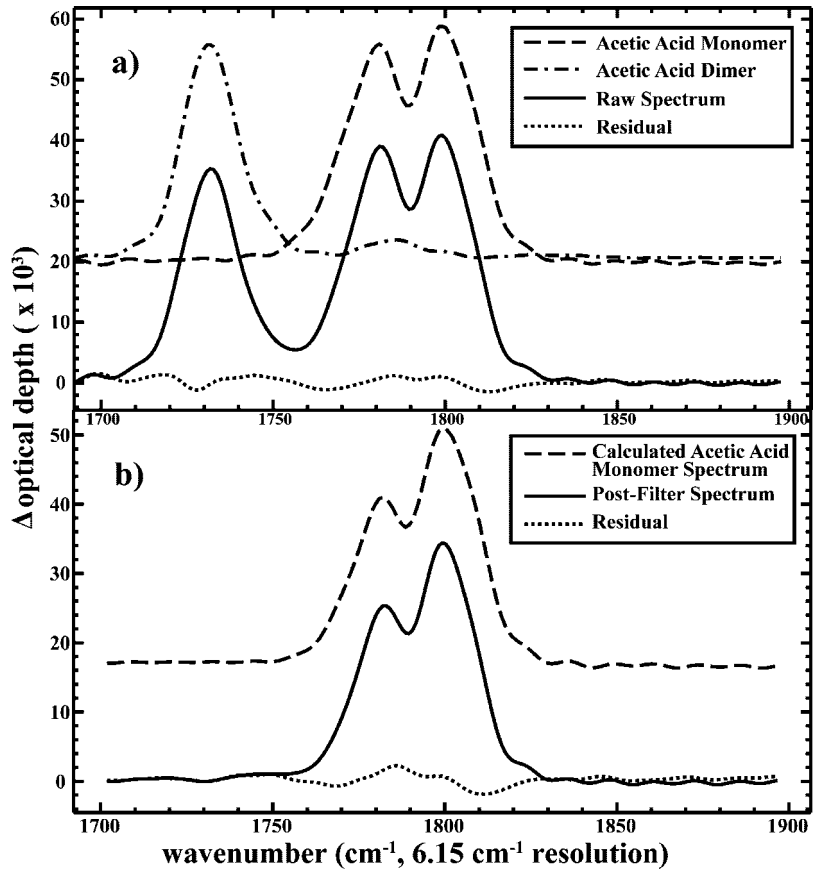

Figure 1. (a) Acetic acid monomer and dimer in the spectrum and the correlation analysis result. The solid line is the raw spectrum. The dashed line is the calculated acetic acid monomer spectrum. The dash−dot line is the acetic acid dimer spectrum. The dotted line is the residual after subtraction. The concentrations for the monomer and the dimer are 6.30×10^{13} and 1.70×10^{13} molecule cm^{-3}, respectively. (b) The filtered spectrum that only contains the acetic acid monomer feature. The solid line is the filtered spectrum where the dimer feature has been eliminated. The dashed line is the calculated acetic acid monomer spectrum. The dotted line is the residual after subtraction. The concentration of acetic acid monomer is 6.47×10^{13} molecule cm^{-3}.

TABLE 1: Summary of Experimental Conditions and Results

temperature (K)	[acetic acid] (10^{13} molecules cm^{-3})	rate constant (k_1) (10^{-13} cm^3 $molecule^{-1}$ s^{-1})	pressure	exp no.
256	0.413 − 7.36	9.69 ± 0.32	6.6	8
266	2.33 − 9.34	8.57 ± 0.45	6.5	4
275	2.24 − 10.6	7.79 ± 0.36	6.5	8
286	3.07 − 11.4	6.91 ± 0.13	6.6	7
295	2.00 − 14.0	6.77 ± 0.14	6.6	19
307	2.29 − 11.4	6.26 ± 0.51	6.8	3
315	3.15 − 11.3	5.86	6.8	1
328	3.71 − 14.4	5.27 ± 0.12	6.8	4
338	3.98 − 16.0	4.89 ± 0.09	6.8	4
346	4.31 − 17.0	4.44 ± 0.13	6.8	7
357	4.32 − 22.0	3.99 ± 0.14	6.7	4

of Singleton et al. in the high temperature range, Butkovskaya et al. determined a three-parameter expression for the temperature dependence of OH + CH_3COOH to be: $k_1(T) = (2.45 \times 10^{-16})$ $(T/298)^{5.24 \pm 0.68}$ $\exp((2358 \pm 189)/T)$ cm^3 $molecule^{-1}$ s^{-1}.[12] By use of this expression, a rate constant of 2.2×10^{-12} cm^3 $molecule^{-1}$ s^{-1} is obtained at 220 K, which is greater than the JPL recommendation by Sander et al.[16] On the basis of this faster rate, Butkovskaya et al. estimated a residence time of 9.4 days for CH_3COOH in the upper troposphere assuming an average OH concentration of 5.5×10^5 molecule cm^{-3}.[12] This finding suggests that the OH + CH_3COOH reaction might be an efficient source of methyl peroxy radicals and a net source of HO_x radicals in the upper troposphere. Crunaire et al. used continuous-wave cavity ringdown spectroscopy (cw-CRDS) to study the atmospheric oxidation of acetic acid in a simulation chamber at 760 Torr.[17] They reported a rate constant of $(6.5 \pm 0.5) \times 10^{-13}$ cm^3 $molecule^{-1}$ s^{-1} at 296 K. Vimal and Stevens used the discharge-flow technique with resonance fluorescence detection of the OH radicals to study OH + CH_3COOH at low pressures from 2−5 Torr and 263−373 K.[18]The Arrhenius equation to describe the negative temperature dependence they observed is $k_1(T) = (2.52 \pm 1.22) \times 10^{-14}$ $\exp((1010 \pm 150)/T)$ cm^3 $molecule^{-1}$ s^{-1}, and the rate constant at 300 K is $(7.42 \pm 0.12) \times 10^{-13}$ cm^3 $molecule^{-1}$ s^{-1}. Khamaganov et al. determined the OH + CH_3COOH reaction rate constants at 50 and 100 Torr over the wide temperature range of 287−802 K with pulsed laser photolysis of CH_3COOH to generate OH and pulsed laser-induced fluorescence to detect OH.[19] They observed the mechanistic change

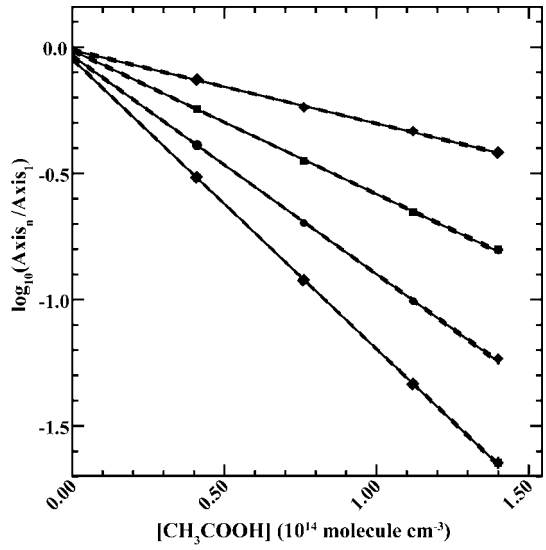

Figure 2. First-order decay plot for the OH signals at 295 K and 6.5 Torr. Different lines represent different LIF detection axes, with the line through the diamonds being the second axis, etc. Note that our x-axis is the acetic acid concentration and that this is a relative decay with respect to detection axis 1.

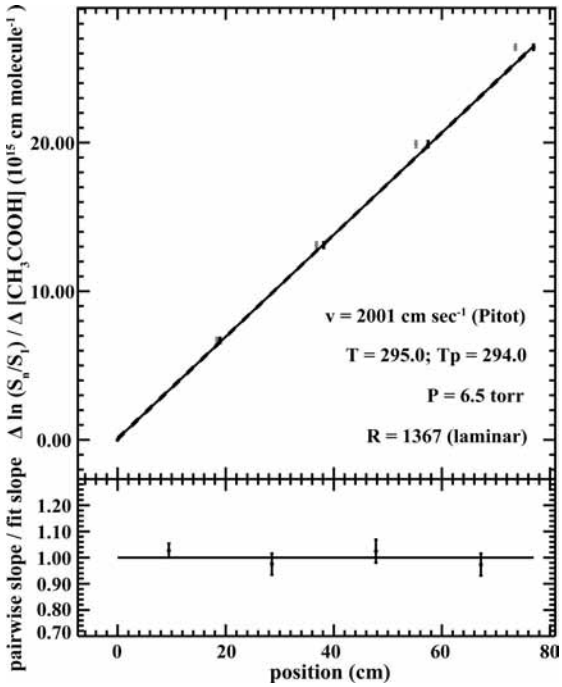

Figure 3. Subsequent rate plot of the decay plot in Figure 2 at 295 K and 6.5 Torr. The rate constant is 6.87×10^{-13} cm^3 molecule^{-1} s^{-1}.

from the dominance of channel 1a to channel 1b at high temperatures. As a result, a sharp minimum occurs in the Arrhenius plot at 530 K, and the temperature dependence of the rate constant can be described as the sum of two Arrhenius equations: $k_1(T) = 2.9 \times 10^{-9} \exp(-6030/T) + 1.50 \times 10^{-13}\exp(515/T)$ cm^3 molecule^{-1} s^{-1}.

The mechanism of the reaction OH with acetic acid has been the focus of a few isotopic studies. Singleton et al. reported a rate constant for OH + CD_3COOH that is similar to the rate of OH + CH_3COOH but a much slower rate for OH + CD_3COOD. This finding suggests that the acidic channel 1a is the major channel. They proposed an adduct formation that involves hydrogen bonding between the carbonyl oxygen of the acid and the hydrogen of the OH radical, accounting for the observed negative temperature dependence. They also concluded that the acetic acid dimer reacts much more slowly toward OH than the monomer.[15] Butkovskaya et al. measured the prompt yield of CO_2, using the chemical ionization mass spectrometer, and determined the branching ratio for the acidic channel to be 64 ± 17% over the temperature range of 249−298 K.[12] De Smedt et al. also experimentally determined the branching ratio for the same channel to be 64 ± 14% at 290 K. The quantum chemical calculations on the potential energy surface of the title reaction performed by De Smedt et al. indicates that the formation of very stable H-bonded pre-reaction complexes greatly enhances the importance of the acidic abstraction channel. They estimate the well depth for the H-bonded pre-reaction complex formation to be −7.3 kcal mol^{-1}.[20] Rosado-Reyes and Francisco studied the atmospheric oxidation pathways of acetic acid theoretically and calculated a well depth of −6.5 kcal mol^{-1}.[21] Crunaire et al. reported 78 ± 13% for the branching ratio for channel 1a.[17] More recently, Sun and Saeys used first-principle calculations and estimated the branching ratio to be 94% and a rate constant of 2×10^{-13} cm^3 molecule^{-1} s^{-1}.[22]

The inability of chemical models to reproduce atmospheric measurements of acetic acid has been known for some time.[23] The inconsistency in the literature in the estimated global photochemical source and the direct emission of acetic acid indicates that the atmospheric chemistry involving acetic acid is not well understood. Hence, a thorough examination of possible sources and loss mechanisms involving acetic acid and a more reliable kinetics data set for use in models are called for. Although several groups have measured the rate of OH + acetic acid and its temperature dependence, the rates differ by 30% even at room temperature, ranging from 6 to 8×10^{-13} cm^3 molecule^{-1} s^{-1}. The disagreement at lower temperatures is as great as 300%, yet these are the temperatures of the upper troposphere and lower stratosphere where this loss mechanism is believed to be most significant Therefore, a reliable measurement of the rate of OH + acetic acid is needed to help improve our understanding of acetic acid and the role it plays in global tropospheric chemistry.

We present here a new set of kinetics data set using our High-Pressure Flow System (HPFS) at ∼7 Torr and over the temperature range of 255−355 K. FTIR spectrometry is used to quantify the acetic acid monomer concentration and allows for low uncertainty measurements. Our data set bridges the gap between the low temperature study by Butkovskaya et al.[12] and the high temperature studies conducted by Dagaut et al.,[14] Singleton et al.,[15] Vimal and Stevens,[18] and Khamaganov et al.[19]

Experimental Section

Our HPFS and the analysis method employed in this study have been described in detail previously.[24−26] A brief summary of the instrument with changes specific to this study is provided here.

The HPFS consists of a 700 L settling chamber followed by a 10 m long, 12.36 cm internal diameter stainless steel pipe that allows the carrier gas flow to fully develop laminar flow before entering the detection zone. System pressure is measured with a calibrated 10 Torr capacitance manometer (MKS). A pitot-static tube is used to measure the velocity of the core of the flow and is connected to a 1 Torr differential capacitance manometer (MKS). The velocity is typically 13−18 m/s. Temperature is measured at the beginning and at the end of the reaction zone in the center of the flow. The kinetic experiments are performed under pseudo-first-order conditions with

TABLE 2: Summary of All Experimental Results of Rate Constant and Arrhenius Parameters of the OH + CH_3COOH Reaction

temperature (K)	pressure (Torr)	k_1 (room T) (10^{-13} cm^3 molecule^{-1}s^{-1})	A (10^{-14} cm^3 molecule^{-1} s^{-1})	$E/R \pm \Delta E/R$ (K)	ref
298	22−500	5.99 ± 0.78			Zetzsch and Stuhl[13]
240−440	25−50	7.40 ± 0.60 (298K)	130 ± 10	170 ± 20	Dagaut et al.[14]
297−446	500	8.67 ± 0.65 (297K)	7.79	−679	Singleton et al.[15]
229−300	200	6.60 ± 1.10 (300K)	2.2 ± 0.2	−1012 ± 80	Butkovskaya et al.[12]
296	760	6.5 ± 0.5			Crunaire et al.[17]
263−373	2−5	7.42 ± 0.12	2.52 ± 1.22	−1010 ± 150	Vimal and Stevens[18]
287−802	50 and 100	8.5 ± 0.9 (296K)	15.0	−515 ± 30	Khamaganov et al.[19]
255−355	6.6	6.77 ± 0.14	5.38 ± 0.28	−740 ± 51	This work

CH_3COOH as the excess reagent. Hydroxyl radicals are generated by sending H_2 gas along with Ar through a microwave induced plasma to form H atoms, which are then reacted with NO_2 to make OH radicals via the reaction, H + NO_2 → OH + NO. These radicals are injected into the center of the bulk flow with a quartz injector and detected by laser-induced fluorescence (LIF). The detection zone immediately downstream of the injection site has five equally spaced detection axes. The detection axes have been modified since previous published experiments. The liquid light guides have been removed, and the photomultiplier tubes (PMTs) now rest directly atop each axis, perpendicular to the laser. Because of this change and the addition of telescoping lenses and optical filters attached to the PMTs, the photon collection efficiency is improved, the center of the flow tube imaged better, and the OH sensitivity optimized. The OH sensitivity was calibrated by reacting known amounts of NO_2 with excess H in the injector. The sensitivity for OH signal is ∼5−9 × 10^{-6} counts s^{-1} cm^3 molecule^{-1} mW^{-1} before entering the detection zone depending on the axis. This translates to a detection limit of ∼1 × 10^6 molecule cm^{-3} mW^{-1} (S/N = 1, 1s integration).

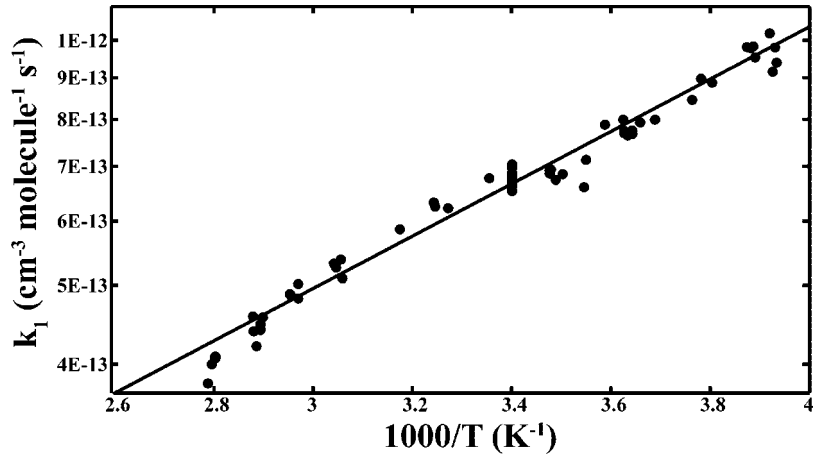

Figure 4. Raw data of the rate constants and the weighted fit.

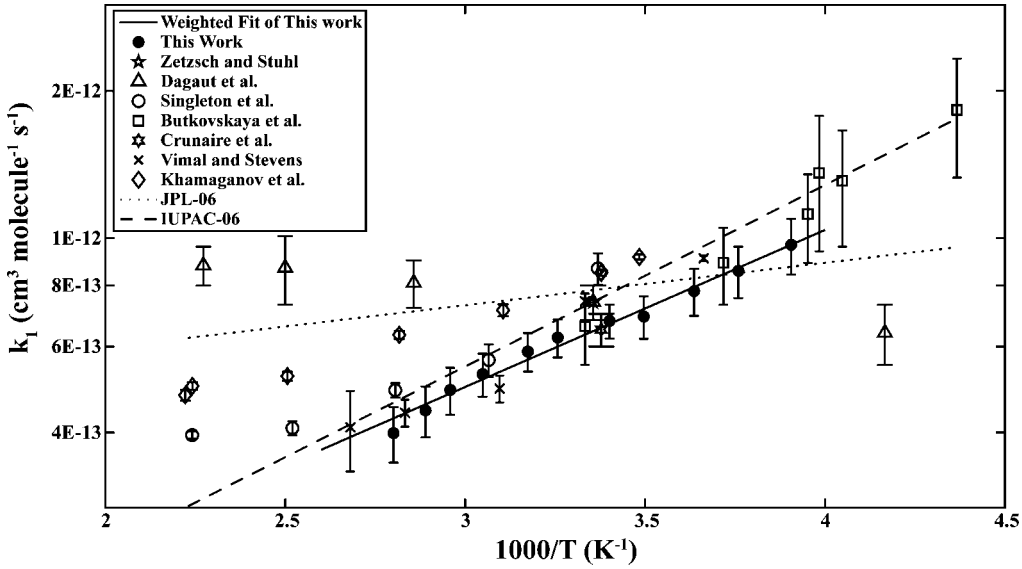

Figure 5. Summary of all experimental data, their errors, and the fits recommended by JPL and IUPAC. The solid line is our fit to our data. The dashed line is the IUPAC-06 recommendation. The dotted line is the JPL-06 recommendation.

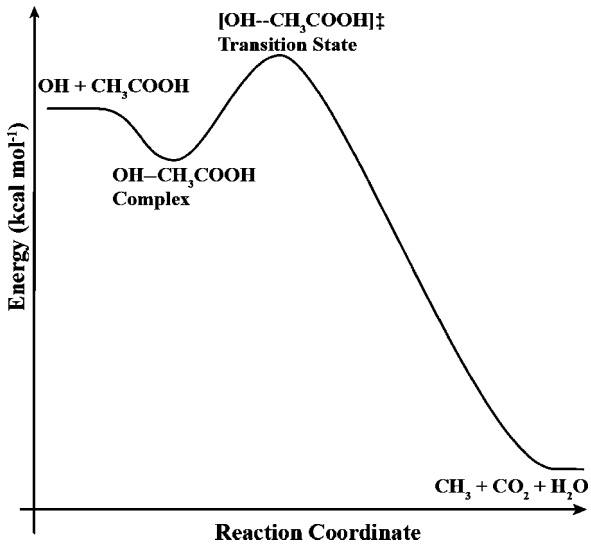

Figure 6. The potential energy surface of the title reaction. The well depth has been calculated to be 7.3 kcal mol^{-1} by De Smedt et al.[20] and 6.5 kcal mol^{-1} by Rosado-Reyes and Francisco[21] below the reactants. However, the experimental fits from both Butkovskaya et al.[12] and Vimal and Stevens[18] yield a well depth of ~2 kcal mol^{-1}, while our data correspond to a well depth of ~1.5 kcal mol^{-1}. The barrier height is uncertain, with De Smedt et al. reporting a range of 1.6−3.3 kcal mol^{-1} and Rosado-Reyes and Francisco reporting it to be 2.1 kcal mol^{-1} above the reactants.[20,21] The products are calculated to be 22.9 kcal mol^{-1} below the reactants according to De Smedt et al.[20] Tunneling is believed to play an important role in going through the transition state.[19,20]

The acetic acid is injected at the beginning of the flow tube immediately after the settling chamber and is measured using a FTIR spectrometer (Mattson) coupled with a 44-pass White cell located between the first two LIF detection axes. The path length of the White cell is calibrated with halocarbon F12 and is 550 cm in this set of experiments. We modulate acetic acid concentrations to reduce our sensitivity to experimental drifts throughout a run. Four different acetic acid concentrations are typically used in one run. Acetic acid concentrations in our flow system are calibrated using the cross sections obtained by Tyndall and Orlando[27] in the mid-IR. Their cross sections agree very well with those reported by Tuazon et al.[28] and Crawford et al.;[29] all agree to within 10%. We fit an acetic acid spectrum taken in the HPFS with the reference spectrum and assign the concentration obtained from the Igor fitting program to that spectrum.

The feature at 1750−1830 cm^{-1} in the acetic acid spectrum is the key feature used in our analysis. The complication to the acetic acid monomer measurement comes in at temperatures below room temperature (~295 K) where acetic acid monomer and dimer are both present, and the fraction of the dimer increases as the temperature decreases. To free the spectrum from dimer complication and obtain the monomer concentration, we use a Gaussian filter to eliminate the spectral region containing the dimer feature. The filter is designed to change the weighting from 1 to 0 smoothly in order to remove the dimer feature while achieving minimal biasing. After the filter is applied to both the reference spectrum and the data spectrum, the resultant spectrum is analyzed to obtain the monomer concentration only. Figure 1a shows a raw spectrum with both the monomer and the dimer feature at 254.4 K, which contains one of the highest concentrations of dimer in the entire data set. A simultaneous correlation analysis yields concentrations of 6.30×10^{13} and 1.70×10^{13} molecule cm^{-3} for the monomer and the dimer, respectively. Figure 1b shows the result of applying the filter to the raw spectrum in Figure 1a and corresponds to a monomer concentration of 6.47×10^{13} molecule cm^{-3}. We use the filter method because of the minimal time and computing power it required in data acquisition and analysis, and because the difference between the correlation analysis and the filter method is no more than 3% even at the highest dimer concentration in our data set.

The HPFS is wrapped externally with resistive heating tape, which is covered with high-grade insulation (TechLite). For high-temperature runs, the HPFS is heated up slowly to obtain temperature gradients smaller than 2 K throughout the detection zone. There are also copper coils wrapped around the HPFS externally. To measure rate constants at low temperatures, we send liquid nitrogen (LN_2) through the copper coil to cool the carrier gas inside the flow tube. We actively control the LN_2 flow through the copper coil to maintain a small temperature gradient throughout each run.

We use a liquid nitrogen boil-off with no further purification for our main carrier flow. Mixtures of 0.5% hydrogen in UHP helium (Scott) and 2% NO_2 in UHP helium (Matheson) are used in OH generation, along with UHP argon (Matheson) as the carrier gas for the OH source. Acetic acid (Mallinckrodt) is purified via freeze−pump−thaw cycles with the middle section retained. The CH_3COOH is transferred into a large glass bulb and filled with N_2 to make a 2% bulb for injection through the excess reagent manifold.

The biggest source of uncertainty below 340 K is from our excess reagent measurement. Combining the errors in the White cell path length, our fitting algorithm and the experimental error in the reference spectrum of acetic acid, we estimate the 2σ uncertainty to be ~10% at room temperature and with slightly larger uncertainties at higher and lower temperatures. At the highest and the lowest temperatures, however, the major contributor to the uncertainty is the velocity measurement due to the acetic acid addition. At high temperatures where the reaction rate is reduced, more acetic acid is needed in the system to produce decays of more than 1 order of magnitude. At low temperatures, though the reaction rate increases, the formation of the dimer reduces the amount of acetic acid monomer that reaches the reaction zone. In both cases, a relatively large flow of acetic acid is injected, causing minor perturbations in system pressure, and thus causing spikes in the velocity measurement. We estimate our 2σ uncertainty of the rate constant measurements at the extreme temperatures to be ~15%.

Results and Discussion

Rate Constant of the OH + CH_3COOH Reaction. Table 1 summarizes the experimental conditions. The rate constants from individual runs are binned and averaged according to temperature. All experiments are performed between 6 and 8 Torr with a flow velocity around 13−18 m/s under pseudo-first-order conditions. The OH decay monitored in our system can be described as follows

$$[\mathrm{OH}]_{\mathrm{axis}_n(n=2-5)} = [\mathrm{OH}]_{\mathrm{axis}_1} \times \exp(-k_1 \times \mathrm{time} \times [\text{acetic acid}]) \quad (2)$$

Figure 2 illustrates a typical pseudo-first-order decay of OH with various acetic acid concentrations at all axes with respect to axis 1. Typically, the OH decay is linear over 1−1.5 orders of magnitude after subtraction of laser scatter. Figure 3 shows the subsequent rate plot based on the decays in Figure 2. To verify that the instrument has no systematic error, we measure

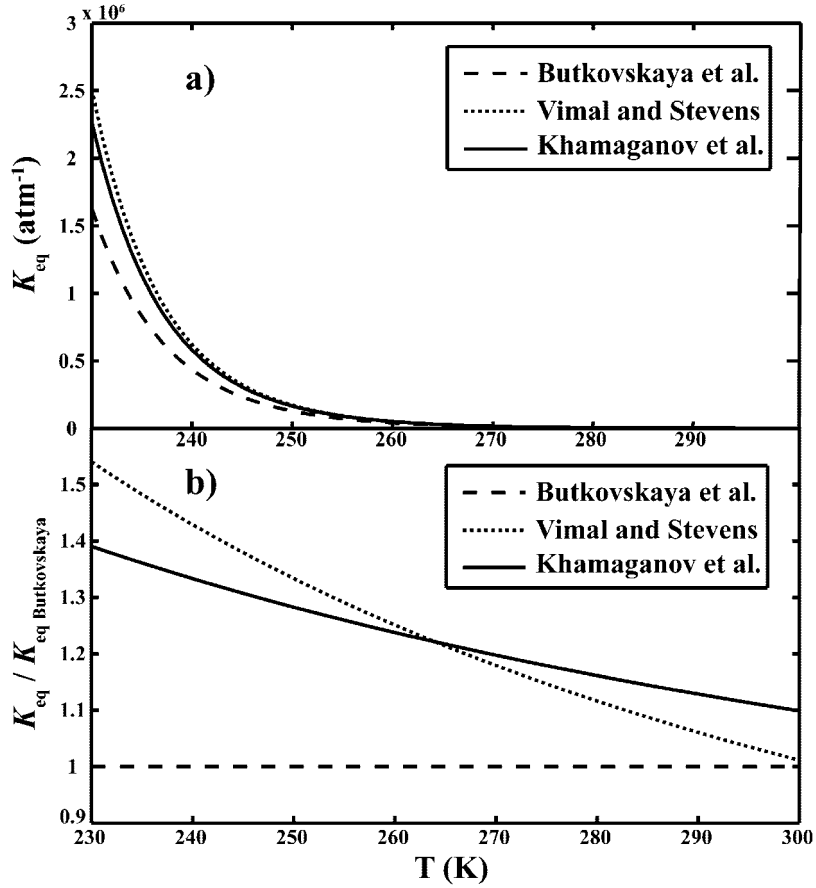

Figure 7. (a) The temperature dependence of the equilibrium constant of acetic acid monomer and dimer. (b) The ratio of K_{eq} with respect to the $K_{eq}$of Butkovskaya et al.

the rate of OH + ethane and/or OH + cyclohexane prior to making the OH + CH_3COOH measurement. All of our measured rates of OH + ethane and OH + cyclohexane agree with earlier measurements on the instrument within ±5% over the entire temperature range.[30,31] The initial OH concentrations are typically $\sim 10^9$ molecules cm^{-3}. The second-order rate constant at 295 K of the OH + acetic acid reaction is $(6.77 \pm 0.14) \times 10^{-13}$ cm^3 $molecule^{-1}$ s^{-1}, in excellent agreement with the rate of $(6.6 \pm 0.8) \times 10^{-13}$ cm^3 $molecule^{-1}$ s^{-1} reported by Butkovskaya et al. at 200 Torr[12] and $(6.5 \pm 0.5) \times 10^{-13}$ cm^3 $molecule^{-1}$ s^{-1} by Crunaire et al. at 760 Torr,[17] and is in good agreement with other studies listed in Table 2, along with the JPL recommended rate constant of 8.0×10^{-13} cm^3 $molecule^{-1}$ s^{-1}.[16] Table 2 also summarizes all the experimental kinetics results and the reported Arrhenius parameters.

Figure 4 shows all of our raw data and the fit for the temperature dependence of the rate constant of OH reacting with acetic acid. A weighted fit of our measurements of the rate constant yields the following Arrhenius expression: $(5.38 \pm 0.28) \times 10^{-14}$ exp $(740 \pm 51/T)$ cm^3 $molecule^{-1}$ s^{-1}. This result is in good agreement with the fits obtained by Vimal and Stevens in the high temperature end (320−360K)[18] and by Butkovskaya et al. at $T \leq 300$K.[12] Since Butkovskaya et al. report a ± 26% uncertainty at 247 K, the difference between our fit and their fit is within the combined uncertainties. Figure 5 shows all the experimental data on the title reaction, their associated errors and the fits recommended by JPL[16] and IUPAC.[32] The recommendation from the JPL panel evaluation has not changed since 2002; so recent data[12,17−19] have not been considered, and the slope of the fit appears to be less steep, consequently less sensitive to changes in temperature.

Our fit result of $(5.38 \pm 0.28) \times 10^{-14}$ exp $(740 \pm 51/T)$ cm^3 $molecule^{-1}$ s^{-1} corresponds to a negative activation energy of ~1.5 kcal mol^{-1}, which is similar to the 2 kcal mol^{-1} obtained by Butkovskaya et al.[12] and Vimal and Stevens.[18] The negative temperature dependence suggests that a pre-reactive complex forms between the OH radical and the acetic acid monomer. This finding is consistent with previously reported results.[12,15,18,19]

Even though we have not addressed the pressure dependence in our study, the similarity in results in the temperature dependence among our data, the data of Vimal and Stevens at 5 Torr,[18] and the data of Butkovskaya et al. at 200 Torr[12] suggests that even at a pressure as low as 5 Torr, the rate constant of the title reaction may very well be in the high-pressure limit. Figure 6 illustrates the potential energy surface for this reaction.

The Role of the Equilibrium Constant of the Dimer and the Monomer in Acetic Acid Quantification. In previous temperature-dependent kinetic studies, the acetic acid concentrations have been determined by flow[14,15,18,19] along with single wavelength absorption spectroscopy.[12] These methods rely on equilibrium constants to yield the concentrations of the monomer and the dimer respectively. Depending on the equations used and the accuracy of the temperature measurement, the equilibrium constant could be drastically different, which results in different acetic acid concentrations. In pseudo-first-order kinetic experiments, the concentration of acetic acid is taken as a constant when extracting the rate constant, so any error in the acetic acid measurement directly impacts the quality of the rate constant measurement.

The accuracy of the equilibrium constant (K_{eq}) is dependent on the accuracy of the temperature measurement, which could

lead to high uncertainty in the monomer measurement, especially at low temperatures where the dimer to monomer ratio increases sharply. Moreover, the equation that describes the temperature dependence of the equilibrium constant between the monomer and the dimer varies dramatically depending on the source or the extrapolation. Butkovskaya et al., Vimal and Stevens, and Khamaganov et al. have used three different expressions for the equilibrium constants to help determine the acetic acid concentration in their low-temperature kinetics measurements.[12,18,19] Butkovskaya et al. used the expression: $K_{eq}(T)$ $(atm^{-1}) = [D]/[M]^2 = (2.80 \times 10^{-8}) \exp(7290/T)$.[12,33,34] Vimal and Stevens relied on the expression from the absorption study by Orlando and Tyndall: $K_{eq}(T)$ $(atm^{-1}) = [D]/[M]^2 = (7.1 \times 10^{-9}) \exp(7705/T)$.[18,29,35,36] Khamaganov et al. derived a fit from the data of Chao and Zwolinski and arrived at the expression: $\ln K_{eq}(T) = -18.07 \pm 0.05) + (7522 \pm 17)/T$.[19,35]

Parts a and b of Figure 7 demonstrate how the difference in the three equations for $K_{eq}(T)$ increases steeply with decreasing temperature due to the exponential nature of the equation. Therefore, a small error in temperature measurement could have huge impact on the monomer concentration. Moreover, the choice of equation to define $K_{eq}(T)$ can result in a difference as large as 24% in the acetic acid monomer measurement at 230 K, if one used that reported by Butkovskaya et al. instead of by Vimal and Stevens. The dependence of the equilibrium constant on temperature measurement and the choice of equation cause undesired error in the measurement of the concentration of the acetic acid monomer and affect the quality of the rate constant measurement of OH + acetic acid monomer.

While other groups rely on the equilibrium constant to separate the concentrations of the dimer and the monomer respectively, our application of FTIR spectrometry allows us to measure the concentration of the monomer directly and independently of the concentration of the dimer. It is believed that OH has low reactivity toward the dimer because the reactive −COOH sites are engaged in the hydrogen bonds that hold the dimer together.[12,15] At the lowest temperature we operate (255 K), the dimer concentration is only 25% of the monomer concentration. Due to the low reactivity (estimated to be 1000 times smaller than that of the monomer)[12,15,18] and the low proportionality, we are confident that the existence of the dimer does not contribute significantly to our observed OH decay.

Much of the discrepancy between the present data set and those reported by Vimal and Stevens[18] and Khamaganov et al.[19] may be traced back to the choice of the equilibrium constant. Our measurement of acetic acid monomer is the only direct and independent method of the acetic acid monomer measurement, and it greatly reduces the uncertainty in our data.

Conclusion

Experimental finding of a negative temperature dependence of the rate constant of OH + acetic acid monomer in the temperature range of 255−355 K at 7 Torr agrees well with the results of Singleton et al.,[15] Butkovskaya et al.,[12] Vimal and Stevens,[18] and the recent recommendation made by IUPAC[32] but is in contrast to the positive temperature dependence reported by Dagaut et al.[14] and the weak negative temperature dependence recommended by JPL.[16] A proposed pre-reactive hydrogen-bonded complex formation between the OH radical and acetic acid monomer is consistent with the negative temperature dependence finding. The kinetics result suggests a more significant role for acetic acid in controlling the oxidative capacity of the upper troposphere than previously believed. The measurement of the acetic acid monomer concentration using FTIR spectrometry greatly reduces uncertainty in the data below room temperature. In the existing literature, research groups have focused on temperature regions either above or below room temperature. Our data serve to bridge the discontinuity in literature values with low uncertainty. More work is needed at temperatures below 255 K at low pressures to help understand the pressure dependence of the rate constant of the title reaction.

Acknowledgment. The authors would like to thank Dr. Thomas Hanisco for valuable discussions on the calibration. In addition, Yi-wen Huang would like to thank the NASA ESS fellowship program for the financial support.

References and Notes

(1) Andreae, M. O.; Talbot, R. W.; Andreae, T. W.; Harriss, R. C. *J. Geophys. Res.-At.* **1988**, *93*, 1616.
(2) Baboukas, E. D.; Kanakidou, M.; Mihalopoulos, N. *J. Geophys. Res.-At.* **2000**, *105*, 14459.
(3) de Gouw, J. A.; Middlebrook, A. M.; Warneke, C.; Goldan, P. D.; Kuster, W. C.; Roberts, J. M.; Fehsenfeld, F. C.; Worsnop, D. R.; Canagaratna, M. R.; Pszenny, A. A. P.; Keene, W. C.; Marchewka, M.; Bertman, S. B.; Bates, T. S. *J. Geophys. Res.-At.* **2005**, 110.
(4) von Kuhlmann, R.; Lawrence, M. G.; Crutzen, P. J.; Rasch, P. J. *J. Geophys. Res.-At.* **2003**, 108.
(5) Ito, A.; Sillman, S.; Penner, J. E. *J. Geophys. Res.-At.* **2007**, 112.
(6) Ito, A.; Penner, J. E. *J. Geophys. Res.-At.* **2004**, 109.
(7) Talbot, R. W.; Andreae, M. O.; Berresheim, H.; Jacob, D. J.; Beecher, K. M. *J. Geophys. Res.-At.* **1990**, *95*, 16799.
(8) Enders, G.; Dlugi, R.; Steinbrecher, R.; Clement, B.; Daiber, R.; Voneijk, J.; Gab, S.; Haziza, M.; Helas, G.; Herrmann, U.; Kessel, M.; Kesselmeier, J.; Kotzias, D.; Kourtidis, K.; Kurth, H. H.; McMillen, R. T.; Roider, G.; Schurmann, W.; Teichmann, U.; Torres, L. *Atmos. Environ. A* **1992**, *26*, 171.
(9) Kawamura, K.; Ng, L. L.; Kaplan, I. R. *Environ. Sci. Technol.* **1985**, *19*, 1082.
(10) Warneck, P. *J. Atmos. Chem.* **2005**, *51*, 119.
(11) Jacob, D. J.; Heikes, B. G.; Fan, S. M.; Logan, J. A.; Mauzerall, D. L.; Bradshaw, J. D.; Singh, H. B.; Gregory, G. L.; Talbot, R. W.; Blake, D. R.; Sachse, G. W. *J. Geophys. Res.-At.* **1996**, *101*, 24235.
(12) Butkovskaya, N. I.; Kukui, A.; Pouvesle, N.; LeBras, G. *J. Phys. Chem. A* **2004**, *108*, 7021.
(13) Zetzsch, C. S., F. Proceedings of the 2nd European Symposium on the Physico-Chemical Behaviour of Atmospheric Pollutants, Dordrecht, Holland, 1982.
(14) Dagaut, P.; Wallington, T. J.; Liu, R. Z.; Kurylo, M. J. *Int. J. Chem. Kinet.* **1988**, *20*, 331.
(15) Singleton, D. L.; Paraskevopoulos, G.; Irwin, R. S. *J. Am. Chem. Soc.* **1989**, *111*, 5248.
(16) Sander, S. P.; Friedl, R. R.; Golden, D. M.; Kurylo, M. J.; Moortgat, G. K.; Wine, P. H.; Ravishankara, A. R.; Kolb, C. E.; Molina, M. J.; Finlayson-Pitts, B. J.; Huie, R. E.; Orkin, V. L. Chemical Kinetics and Photochemical Data for Use in Atmospheric Studies: Evaluation number 15; Jet Propulsion Laboratory: Pasadena, CA, 2006.
(17) Crunaire, S.; Tarmoul, J.; Fittschen, C.; Tomas, A.; Lemoine, B.; Coddeville, P. *Appl. Phys. B* **2006**, *85*, 467.
(18) Vimal, D.; Stevens, P. S. *J. Phys. Chem. A* **2006**, *110*, 11509.
(19) Khamaganov, V. G.; Bui, V. X.; Carl, S. A.; Peeters, J. *J. Phys. Chem. A* **2006**, *110*, 12852.
(20) De Smedt, F.; Bui, X. V.; Nguyen, T. L.; Peeters, J.; Vereecken, L. *J. Phys. Chem. A* **2005**, *109*, 2401.
(21) Rosado-Reyes, C. M.; Francisco, J. S. *J. Phys. Chem. A* **2006**, *110*, 4419.
(22) Sun, W.; Saeys, M. *J. Phys. Chem. A* **2008**, *112*, 6918.
(23) Sommariva, R.; de Gouw, J. A.; Trainer, M.; Atlas, E.; Goldan, P. D.; Kuster, W. C.; Warneke, C.; Fehsenfeld, F. C. *Atmos. Chem. Phys. Discuss.* **2008**, 8.
(24) Abbatt, J. P. D.; Demerjian, K. L.; Anderson, J. G. *J. Phys. Chem.* **1990**, *94* (11), 4566.
(25) Donahue, N. M.; Clarke, J. S.; Demerjian, K. L.; Anderson, J. G. *J. Phys. Chem.* **1996**, *100*, 5821.
(26) Donahue, N. M.; Dubey, M. K.; Mohrschladt, R.; Demerjian, K. L.; Anderson, J. G. *J. Geophys. Res.-At.* **1997**, *102*, 6159.
(27) Tyndall, G. S.; Orlando, J. J., personal communication.
(28) Tuazon, E. C.; Aschmann, S. M.; Atkinson, R.; Carter, W. P. L. *J. Phys. Chem. A* **1998**, *102*, 2316.
(29) Crawford, M. A.; Wallington, T. J.; Szente, J. J.; Maricq, M. M.; Francisco, J. S. *J. Phys. Chem. A* **1999**, *103*, 365.

(30) Clarke, J. S.; Kroll, J. H.; Donahue, N. M.; Anderson, J. G. *J. Phys. Chem. A* **1998**, *102*, 9847.

(31) Michele, M.; Sprengnether, T. J. D.; Clarke, J. S.; Demerjian, K. L.; Donahue, N. M.; Anderson, J. G. "Reaction Rates of Nine C6-C9 Alkanes with OH from 230−379 K: Chemical Tracers for [OH]". In preparation.

(32) Atkinson, R.; Baulch, D. L.; Cox, R. A.; Crowley, J. N.; Hampson, R. F.; Hynes, R. G.; Jenkin, M. E.; Rossi, M. J.; Troe, J. *Atmos. Chem. Phys.* **2006**, *6*, 431.

(33) Hasse, H.; Schmitt, M."Vapour-Liquid Equilibria of System II," 2001.

(34) Gmehling, J.; Onken, U.; Arlt, W.; Grenzheuser, P.; Weidlich, U.; Kolbe, B.; Rarey, J. *Vapour-Liquid Equilibrium Data Collection*; Dechema, Frankfurt, 2002.

(35) Chao, J.; Zwolinski, B. J. *J. Phys. Chem. Ref. Data* **1978**, *7*, 363.

(36) Orlando, J. J.; Tyndall, G. S. *J. Photochem. Photobiol. A* **2003**, *157*, 161.

JP808627W